Int. J. Heat Mass Transfer. Vol. 36, No. 11, pp. 2891–2898, 1993
Printed in Great Britain

0017–9310/93 $6.00 + 0.00

Numerical analysis for hyperbolic heat conduction

HAN-TAW CHEN and JAE-YUH LIN
Department of Mechanical Engineering, National Cheng Kung University, Tainan, Taiwan 701, R.O.C.

(*Received* 12 *June* 1992 *and in final form* 18 *August* 1992)

Abstract—A new numerical simulation of the hyperbolic heat conduction problem is investigated. The primary difficulty encountered in the numerical solution of such a problem is numerical oscillations in the vicinity of sharp discontinuities. In this work, it is shown that the hybrid technique based on the Laplace transform and control volume methods can successfully be applied to suppress these oscillations. The Laplace transform method is used to remove the time-dependent terms, and then the transformed equations are discretized by the control volume scheme. Various comparative examples involving a nonlinear problem with surface radiation and the hyperbolic heat conduction in a composite region are illustrated to verify the accuracy of the present method. Due to the application of the Laplace transform method, the present technique does not need to consider the effects of the Courant number on the numerical results.

INTRODUCTION

IT IS WELL known that the solution obtained from the classical Fourier heat conduction equation exhibits infinite propagation velocity of thermal waves. Despite this physically unrealistic notion of instantaneous energy diffusion, the Fourier heat conduction equation gives quite excellent approximations for most engineering applications. However, this classical heat conduction theory breaks down when one is interested in transient heat flow in an extremely short period of time or for very low temperatures near absolute zero, such as cryogenic engineering, laser-aided material processing, the high-intensity electromagnetic irradiation of a solid and the high-rate heat transfer in rarefied media [1]. Under these circumstances, the theory with the finite propagation velocity of thermal wave will become dominant. Thus a more precise heat flux model needs to be postulated. Vernotte [2] and Cattaneo [3] suggested a modified heat flux model in 1958. Successively, various problems involving the hyperbolic heat conduction have been solved by using various analytical and numerical schemes [4–14]. However, it is difficult to apply the analytical scheme to investigate problems with a complicated geometry or with variable thermal properties. This explains why there has been a growing interest in the numerical scheme for the hyperbolic heat conduction in recent years [4]. The major difficulty encountered in the numerical solution of such problems is numerical oscillations in the vicinity of sharp discontinuities. Carey and Tsai [4] applied the central and backward difference schemes to examine error oscillations for the numerical solution of propagating heat waves reflected at a boundary. Spurious oscillations for the central difference and the excessive diffusions for the backward difference in the solutions can be observed. Glass *et al.* [5] used MacCormack's predictor–corrector scheme to solve the same one-dimensional problem. The accuracy was substantially increased when compared to that of Carey and Tsai [4]. However, we can still observe some numerical oscillations in the vicinity of sharp discontinuities. Furthermore, in their work [5] the numerical calculations are performed by using 1000 mesh intervals and a Courant number of about unity. Subsequently, Glass *et al.* [6] also used the same technique to solve hyperbolic heat conduction with surface radiation. As stated by the authors [6], due to the presence of nonlinear terms in the problem, a smaller Courant number was required to decrease the number and amplitude of numerical oscillations. On the other hand, the larger the nonlinearity, the smaller the value of the Courant number. However, with a decrease in the value of the Courant number, the number and amplitude of numerical oscillations increased because the magnitude of the truncated error terms increased. Thus the modified equation must be used. It is a pity that their numerical results [6] still contained the oscillatory spike at the wave front. Additionally, in their work 1000 time steps were used to compute the hyperbolic solutions. Tamma and Railkar [7] were successful in overcoming sharp discontinuities by using specially tailored transfinite-element formulations. They used the general solution of the transformed equation as the shape function in their formulations. But, the authors did not show that the general solution for other specific problems cannot be found, such as nonlinear problems. Maybe, due to the above reason, Tamma and D'Costa [8] introduced the other technique based on the Galerkin finite element method and the mixed implicit–explicit scheme to analyze hyperbolic heat conduction problems. All illustrated examples evaluated in this paper [8] employed a refined mesh of 500 linear two-noded elements with $\Delta t = 0.001$. Yang [9] applied the

NOMENCLATURE

c	propagation velocity of thermal wave	s	Laplace transform parameter
c_p	specific heat	T	temperature
E_r	dimensionless radiation parameter	t	time
F	dimensionless surface heat flux	x	space variable.
$\tilde{F}$	dimensionless surface heat flux in the transform domain		
f	surface heat flux	Greek symbols	
f_r	reference heat flux	α	thermal diffusivity, $k/\rho c_p$
g	heat source	α_s	surface absorptivity
G	dimensionless heat source, $4\alpha g/cf_r$	η	dimensionless space variable, $cx/2\alpha$ or $c_1x/2\alpha_1$
k	thermal conductivity	θ	dimensionless temperature, $Tkc/\alpha f_r$
l	dimensionless distance between two nodes	$\tilde{\theta}$	dimensionless temperature in the transform domain
l^*	width of pulsed energy source	λ	$(s^2+2s)^{1/2}$
q	heat flux	ξ	dimensionless time, $c^2t/2\alpha$ or $c_1^2t/2\alpha_1$
Q	dimensionless heat flux, q/f_r	ρ	density
$\tilde{Q}$	dimensionless heat flux in the transform domain	σ	Stefan–Boltzmann constant.

characteristic method in conjunction with the high-order total variation diminishing schemes to suppress numerical oscillations. It can be seen from his work that a finer grid was still required.

In the numerical computation of this scheme, the value of the Courant number was 0.4, but the number of control volume cells varied with the investigated problems. In their illustrative problems the number of control volume cells was 100 and 400, respectively. The purpose of the present study is to provide an alternative approach for determining an accurate solution of hyperbolic heat conduction problems without numerical oscillations. In the present formulation, the Laplace transform method is used to remove the time-dependent terms from the governing equations, and then the discretized expression of the transformed equations is derived by using the control volume method. The shape function within the ith control volume $[x_{i-1}, x_{i+1}]$ is derived from the associated homogeneous equation of the transformed equation. It is obvious that this technique is different from that of Tamma and Railkar [7].

MATHEMATICAL FORMULATION

The one-dimensional energy conservation equation is given by

$$\rho c_p \frac{\partial T}{\partial t} = -\frac{\partial q}{\partial x} + g(x,t) \tag{1}$$

where ρ is the density of the medium, c_p the specific heat, q the heat flux and g the heat source term per unit volume.

To accommodate the finite propagation speed of the observed thermal waves, Vernotte [2] and Cattaneo [3] formulated a modified heat flux description in the form

$$\tau \frac{\partial q}{\partial t} + q = -k\frac{\partial T}{\partial x} \tag{2}$$

where τ is a relaxation parameter and is defined as

$$\tau = \frac{\alpha}{c^2} = \frac{k}{\rho c_p c^2} \tag{3}$$

where c is the propagation speed of the thermal wave.

For convenience of numerical analysis, the following dimensionless parameters are introduced:

$$\eta = \frac{cx}{2\alpha}, \quad \xi = \frac{c^2 t}{2\alpha}, \quad \theta = \frac{Tkc}{\alpha f_r},$$

$$Q = \frac{q}{f_r} \quad \text{and} \quad G = \frac{4\alpha g}{c f_r} \tag{4}$$

where x is the space variable and f_r a reference heat flux.

Thus equations (1) and (2) are now given in the dimensionless form as

$$\frac{\partial \theta}{\partial \xi} = -\frac{\partial Q}{\partial \eta} + \frac{G}{2} \tag{5}$$

and

$$\frac{\partial Q}{\partial \xi} + 2Q = -\frac{\partial \theta}{\partial \eta}. \tag{6}$$

Elimination of the dimensionless heat flux Q between equations (5) and (6) leads to a dimensionless description of the hyperbolic heat conduction equation as

$$\frac{\partial^2 \theta}{\partial \xi^2} + 2\frac{\partial \theta}{\partial \xi} = \frac{\partial^2 \theta}{\partial \eta^2} + \frac{1}{2}\frac{\partial G}{\partial \xi} + G. \tag{7}$$

In all illustrative examples of this paper, the dimensionless initial conditions are given by

$$\theta(0,\eta)=0$$
$$\frac{\partial\theta}{\partial\xi}(0,\eta)=0. \tag{8}$$

Various types of the boundary conditions will be discussed in the following individual examples.

SOLUTION METHOD

To remove the ξ-dependent terms, taking the Laplace transform of equation (7) with respect to ξ gives

$$\frac{d^2\tilde{\theta}}{d\eta^2}-(s^2+2s)\tilde{\theta}+\left(\frac{s}{2}+1\right)\tilde{G}=0 \tag{9}$$

where s is the Laplace transform parameter. $\tilde{\theta}$ is the Laplace transform of the dimensionless temperature θ and is defined as

$$\tilde{\theta}(\eta,s)=\int_0^\infty e^{-s\xi}\,\theta(\eta,\xi)\,d\xi. \tag{10}$$

As stated by Tamma and Railkar [7], the selection of the shape functions in the transform domain that are functions of the space variables is an important step for accurately predicting the propagation of thermal waves. Maybe the shape function in the transform domain can arbitrarily be chosen for general thermal problems. However, the selection of the shape functions in the transform domain should be careful for certain special problems, such as the hyperbolic heat conduction model. Otherwise, a poor selection of the shape function will affect the accuracy of the numerical results. This fact will be presented in the first illustrative example of this paper. The following illustration will describe its basic concepts. First, consider the associated homogeneous second-order ordinary differential equation of the form as:

$$\frac{d^2\tilde{\theta}}{d\eta^2}-\lambda^2\tilde{\theta}=0 \quad \eta_i\leqslant\eta\leqslant\eta_{i+1}, \quad i=1,2,\ldots,n-1 \tag{11}$$

where $\lambda=(s^2+2s)^{1/2}$. The following simple notations must be used:

$$\tilde{\theta}(\eta_i)=\tilde{\theta}_i, \quad \tilde{\theta}(\eta_{i+1})=\tilde{\theta}_{i+1} \quad \text{and} \quad l=\eta_{i+1}-\eta_i. \tag{12}$$

The analytical solution of equation (11) in the interval $[\eta_i,\eta_{i+1}]$ with boundary condition (12) is

$$\begin{aligned}\tilde{\theta}(\eta)&=\frac{1}{\sinh(\lambda l)}[\sinh(\lambda(\eta_{i+1}-\eta))\tilde{\theta}_i\\&\quad+\sinh(\lambda(\eta-\eta_i))\tilde{\theta}_{i+1}]\\&=N_1(\eta_{i+1})\tilde{\theta}_i+N_2(\eta_i)\tilde{\theta}_{i+1}\end{aligned} \tag{13}$$

where $N_1(z)$ and $N_2(z)$ are denoted as the hyperbolic shape functions and are given by

$$N_1(z)=\frac{\sinh[\lambda(z-\eta)]}{\sinh(\lambda l)}, \quad N_2(z)=\frac{\sinh[\lambda(\eta-z)]}{\sinh(\lambda l)}. \tag{14}$$

Similarly, the analytical solution of equation (11) in the interval $[\eta_{i-1},\eta_i]$ is

$$\tilde{\theta}(\eta)=N_1(\eta_i)\tilde{\theta}_{i-1}+N_2(\eta_{i-1})\tilde{\theta}_i. \tag{15}$$

It is evident that the selection of the hyperbolic shape function in the present scheme is not the general solution of the governing differential equation (9). Moreover, this basic concept is also different from that of Tamma and Railkar [7].

Integration of equation (9) within the ith control volume $[\eta_{i-1/2},\eta_{i+1/2}]$ can be written as

$$\int_{\eta_{i-1/2}}^{\eta_{i+1/2}}\left[\frac{d^2\tilde{\theta}}{d\eta^2}-\lambda^2\tilde{\theta}+\left(\frac{s}{2}+1\right)\tilde{G}(\eta)\right]d\eta=0 \tag{16}$$

where $\eta_{i+1/2}=(\eta_i+\eta_{i+1})/2$.

It is evident that equation (16) can be rewritten as

$$\left.\frac{d\tilde{\theta}}{d\eta}\right|_{\eta_{i+1/2}}-\left.\frac{d\tilde{\theta}}{d\eta}\right|_{\eta_{i-1/2}}-\lambda^2\int_{\eta_{i-1/2}}^{\eta_{i+1/2}}\tilde{\theta}\,d\eta=-\left(\frac{s}{2}+1\right)\int_{\eta_{i-1/2}}^{\eta_{i+1/2}}\tilde{G}(\eta)\,d\eta. \tag{17}$$

Inserting the approximation for $\tilde{\theta}$, equations (13) and (15), and evaluating the resulting integral produces the following discretized form:

$$\tilde{\theta}_{i-1}-2\cosh(\lambda l)\tilde{\theta}_i+\tilde{\theta}_{i+1}=-\frac{\sinh(\lambda l)}{\lambda}\left(\frac{s}{2}+1\right)\int_{\eta_{i-1/2}}^{\eta_{i+1/2}}\tilde{G}(\eta)\,d\eta. \tag{18}$$

The hyperbolic functions, $\cosh(\lambda l)$ and $\sinh(\lambda l)$, in equation (18) can be expressed in a series form as

$$\cosh(\lambda l)=1+\frac{1}{2!}(\lambda l)^2+O(\Delta(\lambda l)^4) \tag{19}$$

and

$$\sinh(\lambda l)=\lambda l+O(\Delta(\lambda l)^3). \tag{20}$$

With the respective errors of $O(\Delta(\lambda l)^4)$ and $O(\Delta(\lambda l)^3)$ for $\cosh(\lambda l)$ and $\sinh(\lambda l)$, the finite-difference form of equation (18) can be written as

$$\tilde{\theta}_{i-1}+(-2-\lambda^2l^2)\tilde{\theta}_i+\tilde{\theta}_{i+1}=-l^2\left(\frac{s}{2}+1\right)\tilde{G}(\eta_i). \tag{21}$$

Equation (21) is just the central-difference formulation of equation (9). Moreover, it also is a special case of equation (18).

Due to the use of the linear shape function, the following approximations are obtained as (see ref. [15])

$$\left.\frac{\mathrm{d}\tilde{\theta}}{\mathrm{d}\eta}\right|_{\eta_{i+1/2}} = \frac{\tilde{\theta}_{i+1}-\tilde{\theta}_i}{l} \quad \text{and}$$

$$\int_{\eta_{i-1/2}}^{\eta_{i+1/2}} \tilde{\theta}\,\mathrm{d}\eta = l\left(\tfrac{1}{8}\theta_{i-1}+\tfrac{3}{4}\theta_i+\tfrac{1}{8}\theta_{i+1}\right). \tag{22}$$

Substituting equation (22) into equation (17) leads to the discretized expression of equation (9) as

$$\left(1-\frac{\lambda^2 l^2}{8}\right)\tilde{\theta}_{i-1}+\left(-2-\frac{3\lambda^2 l^2}{4}\right)\tilde{\theta}_i+\left(1-\frac{\lambda^2 l^2}{8}\right)\tilde{\theta}_{i+1} = -l\left(\frac{s}{2}+1\right)\int_{\eta_{i-1/2}}^{\eta_{i+1/2}} \tilde{G}(\eta)\,\mathrm{d}\eta. \tag{23}$$

The rearrangement of equation (18) or (21) or (23) in conjunction with the prescribed boundary conditions can yield the following vector–matrix equation:

$$[K]\{\tilde{\theta}\} = \{f\} \tag{24}$$

where $[K]$ is an $(n\times n)$ band matrix with complex numbers, $\{\tilde{\theta}\}$ is an $(n\times 1)$ vector representing the transformed nodal temperature and $\{f\}$ is an $(n\times 1)$ vector representing the forcing terms. The nodal dimensionless temperature θ_i can be determined by using the application of the direct Gaussian-elimination algorithm and the numerical inversion of the Laplace transform technique [16].

ILLUSTRATIVE EXAMPLES

Various examples will be investigated as evidence to the accuracy and efficiency of the present numerical scheme for the hyperbolic heat conduction problems. All the computation is performed on a PC with an 80486 microprocessor and the program is written in FORTRAN.

Example 1: *in a semi-infinite body*

This example concerns a one-dimensional hyperbolic heat conduction in a semi-infinite medium with constant thermal properties and with a uniform initial temperature $T = 0$. Suddenly, the wall at $x = 0$ is impulsively stepped to a fixed temperature. In other words, the dimensionless boundary conditions can be written as

$$\theta = 1 \quad \text{at} \quad \eta = 0$$
$$\theta \to 0 \quad \text{as} \quad \eta \to \infty. \tag{25}$$

This problem has been analytically investigated by Baumeister and Hamill [10] using the Laplace transform method. Figure 1 shows a comparison between the analytical solutions of Baumeister and Hamill [10] and the present results with the formulation of equation (18). It can be seen that the present numerical solution agrees well with the analytical solutions and does not exhibit numerical oscillations at the wave front. Figure 2 depicts the difference between the analytical solutions and the numerical results with the formulations of equations (21) and (23). As shown in Fig. 2, the numerical results using the control volume method with a linear shape function and the central-difference method have numerical oscillations at the wave front. Comparison of the dimensionless temperature shown in Figs. 1 and 2 demonstrates that the selection of the shape functions in the transform domain that are functions of the space variables is an important task for accurately predicting the temperature distribution of the hyperbolic heat conduction problem. This comparison also implies that the hyperbolic shape function is a best choice for the present study. Thus the present scheme with the hyperbolic shape function will be applied to solve other illustrative examples to prove its accuracy. The 101-node modelling with the uniform space size is

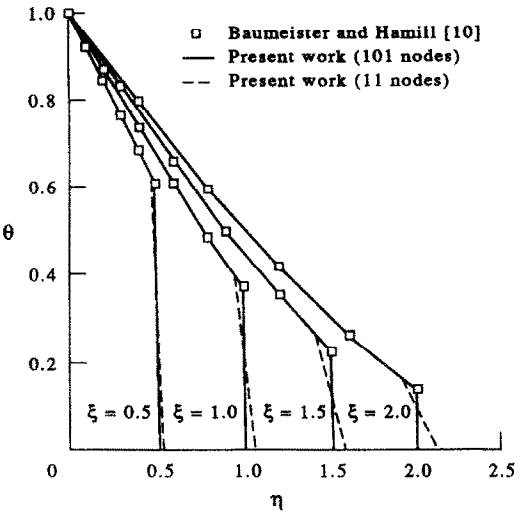

FIG. 1. A comparison of the dimensionless temperature distribution in a semi-infinite medium for various ξ.

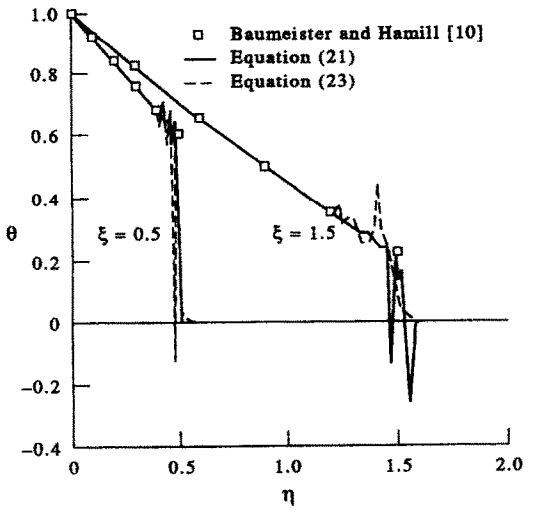

FIG. 2. A comparison of the dimensionless temperature distribution in a semi-infinite medium for various ξ.

Table 1. Practical penetration length for various non-homogeneous materials at $t = \tau$

Material	Thermal diffusivity α (mm^2 s^{-1})	Propagation velocity c (mm s^{-1})	Relaxation parameter τ (s)	Penetration length x (mm)
H acid	0.260	0.103	24.5	2.52
$NaHCO_3$	0.310	0.104	28.7	2.98
Sand	0.408	0.143	20.0	2.85
Glass ballotini	0.251	0.152	10.9	1.65
Ion exchanger	0.220	0.064	53.7	3.44

required for obtaining the numerical results shown in Figs. 1 and 2. In effect, using 11 grid points can also produce excellent results except in the vicinity of sharp discontinuity, as shown in Fig. 1. The reason is that the thermal shock occurs only in an infinitesimal region. Moreover, this infinitesimal region is smaller than the space size in the 11-node modelling. To further prove the accuracy of the present method in conjunction with the finite-difference formulation of equation (18), the following examples will be illustrated by using 101 grid points.

For homogeneous materials, such as pure liquids, gases and dielectric solids, the values of τ range from 10^{-12} to 10^{-8} s [17]. Thus, it can be found from equation (4) that the practical length and time are small for the present problem. However, it can also be found from the work of Kaminski [18] that the values of τ might be significantly larger for materials with a non-homogeneous inner structure. Based on the data of Kaminski [18], Table 1 shows the practical penetration length of the thermal wave at $t = \tau$ ($\xi = 0.5$) for various non-homogeneous materials.

Example 2: *in a finite slab*

This second illustrative problem concerns a finite slab subjected to the dimensionless boundary conditions specified in the following

$$\theta(0, \xi) = 1 \quad \text{and} \quad \frac{\partial \theta}{\partial \eta}(1, \xi) = 0. \tag{26}$$

The analytical solution of this problem has been given by Carey and Tsai [4] using the Laplace transform method. The numerical solutions of this example have also been obtained by Carey and Tsai [4], Glass *et al.* [5] and Tamma and Railkar [7]. Tamma and Railkar [7] can be successful in capturing sharp discontinuities of this problem by using specially tailored transfinite element formulations. In their finite element technique, the hyperbolic shape function is also used as the shape function. But, the shape function chosen by the authors [7] must be the general solution of the hyperbolic heat conduction equation in the transform domain. Thus using the technique proposed by Tamma and Railkar [7] to analyze nonlinear hyperbolic heat conduction problems can be a difficult task. Conversely, the present scheme has not this limitation. It should be noted that the shape functions chosen by Tamma and Railkar [7] are just the same as those shown in the present study only for some linear problems without the source term. Figure 3 shows a comparison of the temperature distribution between the analytical solutions [4] and the present results using the hyperbolic shape function for various dimensionless times. It is seen that excellent agreement is obtained between them. Furthermore, numerical oscillations in the vicinity of sharp discontinuity are also not found in the present results. In particular, the temperature profiles for $\xi = 2$ and 2.5 are interesting. In these cases, the temperatures in the slab are above surface temperature ($\theta = 1$). This phenomenon can classically be admitted for propagating waves, but it is hard to believe that this phenomenon can also occur in a temperature field. Thus Taitel [11] suggested a discrete formulation of the heat conduction equation to explain this dilemma.

Example 3: *with a pulsed energy source*

The third example considers the propagation and reflection of thermal waves in a finite medium with two insulated boundary surfaces and subjected to a pulsed energy source. The pulsed energy source is released instantaneously at $t = 0$, in a region adjacent

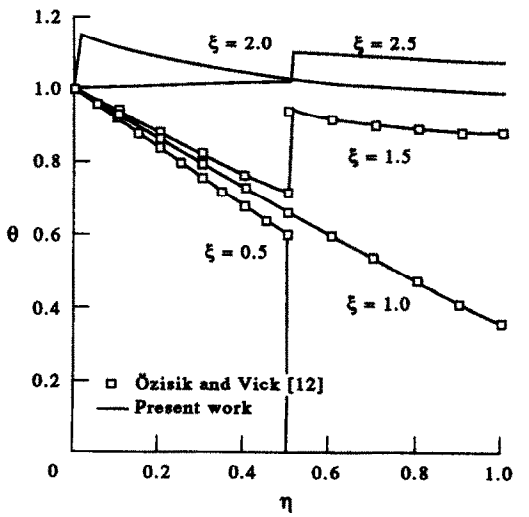

FIG. 3. A comparison of the dimensionless temperature distribution in a slab for various ξ.

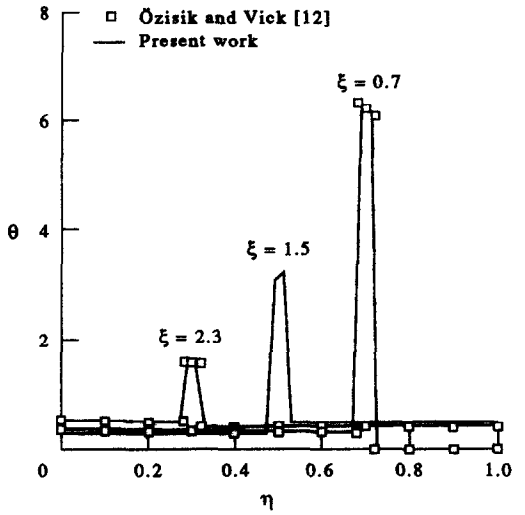

FIG. 4. A comparison of the dimensionless temperature distribution with a pulsed energy source for various ξ.

to the boundary surface at $x = 0$. The dimensionless form of the pulsed energy source can be given by

$$G(\eta, \xi) = \begin{cases} \dfrac{\delta(\xi)}{l^*}, & 0 \leqslant \eta \leqslant l^* \\ 0, & l^* \leqslant \eta \leqslant 1 \end{cases} \quad (27)$$

where $\delta(\xi)$ is the Dirac delta function.

For the numerical calculations, we take $l^* = 0.02$. Özisik and Vick [12] have developed the analytical solutions for the temperature field and heat flux distribution using the finite integral transform. Subsequently, Tamma and Railkar also solved the same problem using the specially tailored transfinite-element method [7]. But, the authors [7] did not show the form of the shape function for this example. Comparison of the dimensionless temperature distribution between the present results using the hyperbolic shape function and the analytical solutions [12] is shown in Fig. 4. The present results are in good agreement with the analytical solutions [12] and do not reveal numerical oscillations in the vicinity of sharp discontinuities.

Example 4: *with surface radiation*

The fourth example is the same as Example 1 except that the left boundary surface at $x = 0$ is subjected to a heat flux $f(t)$ and dissipates heat by radiation into the ambient at temperature T_∞. Thus the boundary condition at $x = 0$ can be written as

$$q = \alpha_s \sigma (T_\infty^4 - T^4) + f(t) \quad \text{at} \quad x = 0 \quad (28)$$

where α_s is the surface absorptivity and σ the Stefan–Boltzmann constant. The following dimensionless parameters are introduced in this example:

$$E_r = \frac{\alpha_s \sigma \alpha^4 f_r^3}{k^4 c^4} \quad \text{and} \quad F(t) = \frac{f(t)}{f_r}. \quad (29)$$

For simplicity, we take $T_\infty = 0$. Thus the dimensionless form of equation (28) can be written as

$$Q = -E_r \theta^4 + F(\xi) \quad \text{at} \quad \eta = 0. \quad (30)$$

The application of the Taylor's series approximation to linearize the nonlinear term θ^4 leads to the linearized form of equation (30) as

$$Q = -E_r(4\bar{\theta}^3\theta - 3\bar{\theta}^4) + F(\xi) \quad \text{at} \quad \eta = 0 \quad (31)$$

where $\bar{\theta}$ is the previously calculated surface temperature. The Laplace transform of equation (31) is

$$\tilde{Q} = -E_r\left(4\bar{\theta}^3\tilde{\theta} - \frac{3\bar{\theta}^4}{s}\right) + \tilde{F}(s). \quad (32)$$

Taking the Laplace transform of equation (6) and substituting equations (13) and (32) into the resulting equation produces the following discretized form:

$$\left[-\cosh(\lambda l) - 4\frac{\sinh(\lambda l)}{\lambda}(s+2)E_r\bar{\theta}_1^3\right]\tilde{\theta}_1 + \tilde{\theta}_2 = -\frac{\sinh(\lambda l)}{\lambda s}(s+2)(3E_r\bar{\theta}_1^4 + 1). \quad (33)$$

In the present problem, the dimensionless boundary heat flux $F(\xi)$ is taken equal to unity. Glass *et al.* [6] utilized MacCormack's predictor–corrector method to solve this example. As stated by them [6], the nonlinearity affects the stability of their scheme. Thus the value of the Courant number used with MacCormack's predictor–corrector methods must be adjusted. Their numerical results still exhibited oscillations near the wave front though. Subsequently, Wu [13] used the Laplace transform method in conjunction with the method of successive approximations to predict the temperature distributions. Wu [13] stated that the selection of the initial approximation must be very close to the analytical solution when the method of successive approximations was applied to solve some higher-order nonlinear problems. The results obtained by Wu [13] did not reveal numerical oscillations in the vicinity of sharp discontinuities. Thus Fig. 5 only shows a comparison of the present results using the hyperbolic shape function with those obtained by Wu [13]. As shown in Fig. 5, there is no remarkable difference between them. This conclusion implies that using the formulation of equation (18) to solve hyperbolic heat conduction problems with surface radiation still has good accuracy.

Example 5: *in composite regions*

The last example considers a hyperbolic heat conduction problem in a two-region composite slab. The left boundary surface at $x = 0$ is kept at a fixed temperature and the right boundary surface is assumed insulated. Thus the dimensionless boundary conditions at these two boundary surfaces can be written as

$$\theta(0, \xi) = 1 \quad \text{and} \quad \frac{\partial \theta}{\partial \eta}(1, \xi) = 0$$

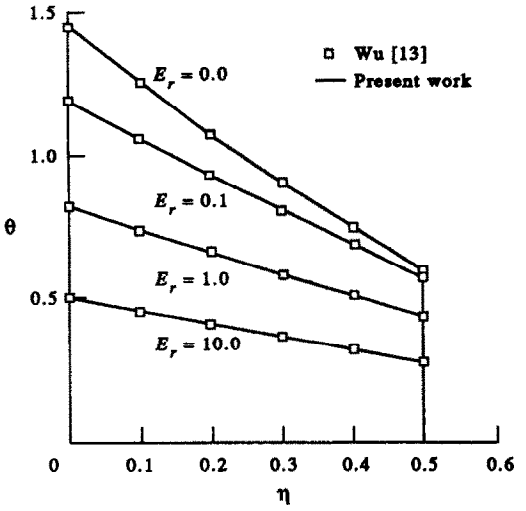

FIG. 5. A comparison of the dimensionless temperature distribution for various E_r at $\xi = 0.5$.

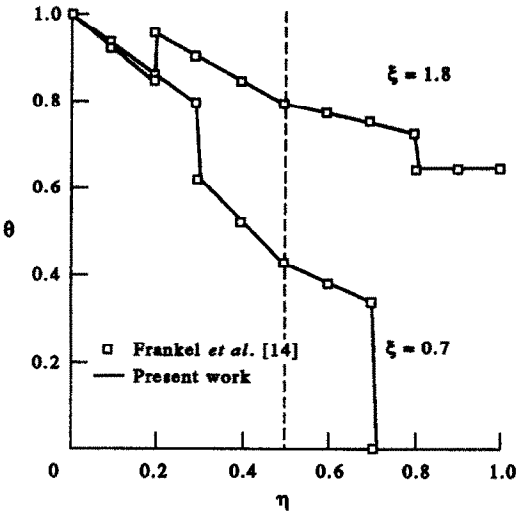

FIG. 6. A comparison of the dimensionless temperature distribution for $\bar{k}_2 = 2$, $\bar{\tau}_2 = 1$ and $\bar{\alpha}_2 = 1$ at $\xi = 0.7, 1.8$.

where ξ and η in this example are again defined as: $\xi = c_1 x/2\alpha_1$ and $\eta = c_1^2 t/2\alpha_1$.

At the interface of the two regions, two boundary conditions are required. Due to the assumption of perfect thermal contact, temperature and heat flux must be compatible at the interface. In other words, two boundary conditions at the interface with the dimensionless parameters of equation (4) can be expressed as

$$\frac{\alpha_1}{k_1 c_1}\theta_1 = \frac{\alpha_2}{k_2 c_2}\theta_2 \quad \text{and} \quad Q_1 = Q_2 \quad \text{at} \quad \eta = \eta_{in}. \tag{34}$$

Thus the dimensionless interface condition using equation (5) can be written as [14]

$$\bar{\tau}_2 \frac{\partial}{\partial \xi}\left(\frac{\partial \theta_1}{\partial \eta}\right) + 2\frac{\partial \theta_1}{\partial \eta} = \bar{k}_2\left[\frac{\partial}{\partial \xi}\left(\frac{\partial \theta_2}{\partial \eta}\right) + 2\frac{\partial \theta_2}{\partial \eta}\right] \quad \text{at} \quad \eta = \eta_{in} \tag{35}$$

where the dimensionless parameters are defined as $\bar{k}_2 = k_2/k_1$, $\bar{\tau}_2 = \bar{\alpha}_2/\bar{c}_2$, $\bar{\alpha}_2 = \alpha_2/\alpha_1$ and $\bar{c}_2 = (c_2/c_1)^2$. It can be seen from equation (35) that the derivative $d\tilde{\theta}/d\eta$ at the interface is not continuous. Taking the Laplace transform of equation (35) and then substituting equations (13) and (15) into the resulting equation leads to the following expression:

$$\left[\frac{\lambda}{\sinh(\lambda l)}(\bar{\tau}_2 s + 2)\right]\tilde{\theta}_{i-1} - \left[\lambda\frac{\cosh(\lambda l)}{\sinh(\lambda l)}(\bar{\tau}_2 s + 2) + \bar{k}_2\lambda_2\frac{\cosh(\lambda_2 l)}{\sinh(\lambda_2 l)}(s+2)\right]\tilde{\theta}_i + \left[\bar{k}_2\frac{\lambda_2}{\sinh(\lambda_2 l)}(s+2)\right]\tilde{\theta}_{i+1} = 0 \quad \text{at} \quad \eta = \eta_{in} \tag{36}$$

where $\lambda_2 = (\bar{\tau}_2 s^2 + 2s)^{1/2}$.

Frankel *et al.* [14] used the generalized finite integral transform technique to analyze this problem. Comparisons between the present results using the formulation of equation (18) and those obtained by Frankel *et al.* [14] are shown in Figs. 6 and 7. Excellent agreements are observed in the figures. The present method using the formulation with the hyperbolic shape function also has good accuracy for hyperbolic heat conduction problems in composite regions.

CONCLUSIONS

The hybrid application of the Laplace transform and control volume methods in conjunction with the

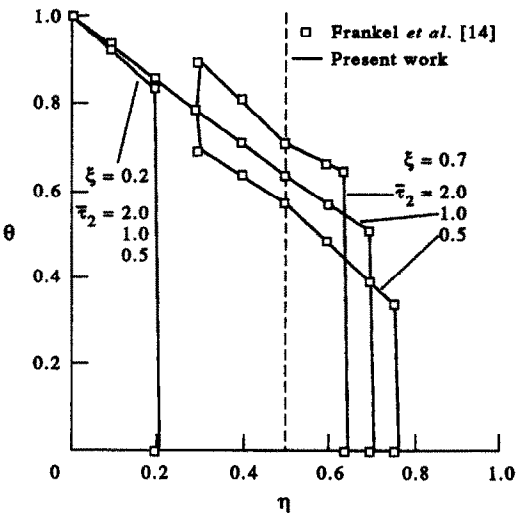

FIG. 7. A comparison of the dimensionless temperature distribution for $\bar{k}_2 = 1$, $\bar{\alpha}_2 = 1$ and various $\bar{\tau}_2$ at $\xi = 0.2, 0.7$.

hyperbolic shape function introduced in this paper provides an excellent result for hyperbolic heat conduction problems. This hyperbolic shape function is obtained by solving the associated homogeneous solution of the transformed equation in the space domain. It is seen from results of five different illustrative examples that this hybrid scheme can give both oscillation-free and highly accurate results. Due to the application of the Laplace transform method with respect to time, the use of the present scheme does not need to consider the effects of the Courant number on the numerical results.

REFERENCES

1. W. W. Yuan and S. C. Lee, Non-Fourier heat conduction in a semi-infinite solid subjected to oscillatory surface thermal disturbances, *J. Heat Transfer* **111,** 178–181 (1989).
2. P. Vernotte, Les paradoxes de la théorie continue de l'équation de la chaleur, *C.R. Acad. Sci.* **246,** 3154–3155 (1958).
3. C. Cattaneo, Sur une forme de l'équation de la chaleur éliminant le paradoxe d'une propagation instantanée, *C.R. Acad. Sci.* **247,** 431–433 (1958).
4. G. F. Carey and M. Tsai, Hyperbolic heat transfer with reflection, *Numer. Heat Transfer* **5,** 309–327 (1982).
5. D. E. Glass, M. N. Özisik, D. S. McRae and B. Vick, On the numerical solution of hyperbolic heat conduction, *Numer. Heat Transfer* **8,** 497–504 (1985).
6. D. E. Glass, M. N. Özisik and B. Vick, Hyperbolic heat conduction with surface radiation, *Int. J. Heat Mass Transfer* **28,** 1823–1830 (1985).
7. K. K. Tamma and S. B. Railkar, Specially tailored transfinite-element formulations for hyperbolic heat conduction involving non-Fourier effects, *Numer. Heat Transfer* **15**(Part B), 211–226 (1989).
8. K. K. Tamma and J. F. D'Costa, Transient modeling/analysis of hyperbolic heat conduction problems employing mixed implicit–explicit α method, *Numer. Heat Transfer* **19**(Part B), 49–68 (1991).
9. H. Q. Yang, Characteristics-based, high-order accurate and nonoscillatory numerical method for hyperbolic heat conduction, *Numer. Heat Transfer* **18**(Part B), 221–241 (1990).
10. K. J. Baumeister and T. D. Hamill, Hyperbolic heat-conduction equation—a solution for the semi-infinite body problem, *J. Heat Transfer* **91,** 543–548 (1969).
11. Y. Taitel, On the parabolic, hyperbolic and discrete formulation of the heat conduction equation, *Int. J. Heat Mass Transfer* **15,** 369–371 (1972).
12. M. N. Özisik and B. Vick, Propagation and reflection of thermal waves in a finite medium, *Int. J. Heat Mass Transfer* **27,** 1845–1854 (1984).
13. C. Y. Wu, Integral equation solution for hyperbolic heat conduction with surface radiation, *Int. Commun. Heat Mass Transfer* **15,** 365–374 (1988).
14. J. I. Frankel, B. Vick and M. N. Özisik, Hyperbolic heat conduction in composite regions, *Proc. 8th Int. Heat Transfer Conf.* (Edited by C. L. Tien *et al.*), Vol. 2, pp. 615–620. San Francisco, California (1986).
15. T. M. Shih, *Numerical Heat Transfer*, pp. 56–57. Hemisphere, New York (1984).
16. G. Honig and U. Hirdes, A method for the numerical inversion of Laplace transforms, *J. Comp. Appl. Math.* **9,** 113–132 (1984).
17. S. Sieniutycz, The variational principle of classical type for non-coupled non-stationary irreversible transport processes with convective motion and relaxation, *Int. J. Heat Mass Transfer* **20,** 1221–1231 (1977).
18. W. Kaminiski, Hyperbolic heat conduction equation for materials with a non-homogeneous structure, *J. Heat Transfer* **112,** 555–560 (1990).